KSME

Springer

Journal of Mechanical Science and Technology 35 (8) 2021

Original Article
DOI 10.1007/s12206-021-0729-3

Keywords:
· Flexible forming
· 3D surface rolling
· Numerical simulation
· Axial radius of roller
· Roll gap distribution
· Longitudinal deformation range

Correspondence to:
Mingzhe Li
limz@jlu.edu.cn

Citation:
Wang, X., Li, M., Liu, Y., Chang, X., Yang, W. (2021). Influence of the axial radius of rigid arc-shaped rollers in 3D surface rolling. Journal of Mechanical Science and Technology 35 (8) (2021) 3579~3589. http://doi.org/10.1007/s12206-021-0729-3

Received October 13th, 2020
Revised April 23rd, 2021
Accepted May 6th, 2021

† Recommended by Editor Hyung Wook Park

Influence of the axial radius of rigid arc-shaped rollers in 3D surface rolling

Xintong Wang[1], Mingzhe Li[1], Yuwei Liu[1,2], Xiang Chang[1] and Weifeng Yang[1]

[1]Dieless Forming Technology Center of Roll Forging Research Institute, College of Materials Science and Engineering, Jilin University (Nanling Campus), Changchun 130022, China, [2]Flight Research Institute, Aviation University of Air Force, Changchun 130022, China

Abstract The research and development of flexible forming technology have a crucial role in the personalized production and manufacturing of three-dimensional (3D) surface sheet metal parts. Three-dimensional surface rolling with rigid arc-shaped rollers (TSRRAR), a new flexible forming technology, was investigated to effortlessly produce 3D surface parts. Numerical simulation and experimental analysis mainly include data at four values of the difference in axial radius of roller (-2, 2, 6 and 10 mm) to explore this technology's forming ability. It was demonstrated that various shapes could be obtained only based on one group of rollers. The maximum resultant force decreased from 3.07 to 2.21 KN, and the required maximum compression rate from 4.22 to 2.48 % with the same longitudinal curvature radius (179 mm) to be obtained. Therefore, the forming difficulty can be reduced by selecting the difference in axial radius of roller.

1. Introduction

In recent years, the products of aviation, aerospace, navigation vehicles, and the new architectural decoration consisting of 3D surface aluminum alloy sheets are increasingly used. The conventional forming methods, such as stamping and hydroforming, are prone to wrinkling, challenging to ensure the curved surface's accuracy, and unsuitable to meet the market demand of small-batch and multi-variety production. Multi-point forming (MPF) has satisfactorily solved similar problems proposed by Li et al. [1]. Many engineering projects, such as the bird's nest building engineering in Beijing, China, have adopted this forming technology for the digital manufacturing of individualized 3D surface parts. However, a multi-point device's manufacturing cost is still high due to a large number of independent control units and the complex control systems, limiting its wider application.

To reduce the processing cost, the equipment and technology having flexible characteristics is an essential requirement, and the processing efficiency is also crucial for forming 3D surface parts. Single point incremental forming [2] and line heating [3], belonging to the category of point forming, have a high degree of flexibility, with the simple forming tool. MPF [4] and flexible stretching forming [5] belong to the category of surface forming. They are more efficient than point forming but the forming equipment is complicated and large, resulting in equipment transportation difficulty. For the 3D surface line forming methods [6-8] still in the development stage, the processing efficiency is obviously higher than others due to the continuous forming process. Besides, the most prominent feature of the method is that when the width of the formed sheet is within the equipment size, there is no size limit on the length.

Some scholars have investigated in depth the 3D surface forming methods based on the category of line forming. Yoon et al. [9] developed a flexible roll forming process. Shim et al. [10] studied the flexible roll forming process by adopting the line array roll set. Li et al. [11] proposed the multi-point continuous roll forming method as a vital branch of multi-point series technologies, which is the combination of multi-point shape-adjusting technology and roll bending technology adopting three working rollers whose shape can be adjusted to continuously

deform sheets. Cai et al. [12] focused on the principle and basic experiment of the flexible roll bending process. Surface flexible rolling (SFR) [13, 14] is also a new continuous and flexible forming method for 3D surfaces. Yoon et al. [15-17] carried out researches on flexible reconfigurable roll forming.

TSRRAR is a new flexible forming method for producing 3D surface sheet metal parts. Since only two working rollers are needed, the equipment is simpler and easier to be controlled than other 3D flexible forming methods based on roll forming. The used working roller has variable cross-sections, which is reflected by the axial radius of roller, and it is a key factor influencing the equipment forming capacity in this study and the flexible forming characteristic as well as the compression rate does in the future study.

This work reports on the forming ability influenced by the axial radius of roller in terms of the technology first proposed in the previous research [18], and the study on process parameters is crucial in plastic forming of sheet metal [19-21]. The novelty of this study is to verify the feasibility of forming various shapes only using one group of rollers by numerical simulation and experimental results, and to achieve the proper combination of the axial radii of convex and concave rolls to effortlessly produce metal sheets, which has reference value for understanding the equipment capacity for forming 3D surface sheet metal parts without changing rollers and adopting rollers capable of slight bending in the future study.

2. Process analysis of TSRRAR

TSRRAR is a new 3D surface continuous forming method that combines the rigid arc-shaped roller and the conventional cold rolling technology. Conventional cold rolling uses rollers whose transverse section line is straight. Whereas the transverse section line of roller in this method is a circle arc, which enables it to produce 3D surface sheet metal parts. This forming method is a different type of rolling because the used rollers are both rigid. The opposite rotation of rollers feeds the sheet, and 3D surface parts with various shapes can be obtained by adjusting the compression rate to sheet metals.

While the deformation principle of TSRRAR is similar to that of SFR, the new technology of using variable cross-section rollers is different and novel which can both ensure the device rigidity and simplify process parameters, thereby ensuring the shape accuracy of roller during the rolling process and making the adjustment process less sensitive and less time-consuming. Therefore, the non-uniform deformation principle adopted in TSRRAR is more practicable than that in SFR to realize the 3D surface forming, which is the benefit of this forming method.

The uneven roll gap with a specific regular distribution is utilized to non-uniformly compress the sheet metal passing, thus achieving the continuous plastic deformation in the rolling direction (longitudinal direction). Besides, deformation occurs under the bending force whose direction is perpendicular to the rolling direction (transverse direction). Finally, a 3D surface part with bending radii in both directions is obtained.

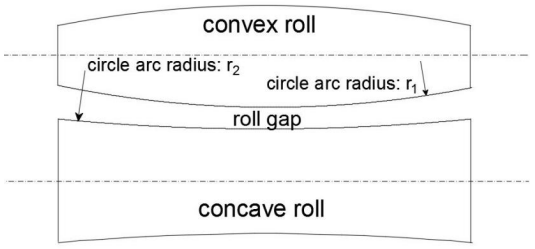

Fig. 1. Definition of the axial radius of roller.

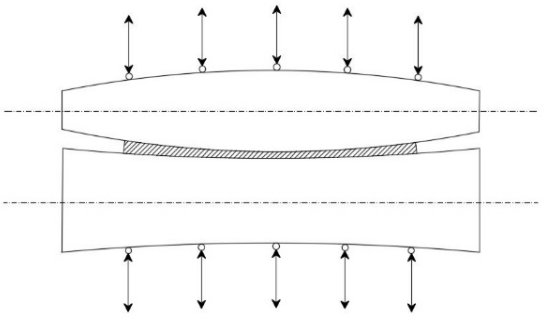

Fig. 2. Schematic diagram of the new 3D surface rolling device.

The intersection between the surface of roller and the transverse middle section is a circle arc. Also, the axial radii of rollers (the circle arc radius of convex roll r_1 and that of concave roll r_2 shown in Fig. 1) need to be reasonably selected according to the sheet size to obtain the target part with a better profile.

First of all, the ultimate goal of the method is to realize flexible forming through parametric flexible control of the rollers, as shown in Fig. 2, and the work in this paper is the prior study on verifying the feasibility of forming various shapes only using one group of rollers.

The flexibility of this study refers to the effect of maximum reduction on the longitudinal deformation of the formed sheet without changing rollers, and the longitudinal curvature radius significantly varies only by a slight change of thickness. Although it is necessary for this forming method to change rollers, there are only a few that need to be prepared for various 3D surfaces because the future study including an advanced equipment with several controlling units along the transverse direction will be designed to realize a slight bending of the roller to be more flexible on the transverse deformation of the formed sheet.

The roll gap distribution of 3D surface rolling is the critical factor affecting the part shape. In order to obtain a 3D surface part, a profit combination of the axial radii of convex and concave rolls is not only critical for the transverse bending radius, but also influences the type of shape of the formed sheet.

Fig. 3 shows the forming process with different distribution rule of roll gap. When it is narrow in the middle and wide on both sides, the metal elongation in the middle of the deformed surface is larger than that on both sides, that is, $\Delta L > \Delta L', \Delta L > \Delta L''$. The forming result in this condition is a

Table 1. Simulation conditions and results of the longitudinal bending radius with various differences in axial radius of concave and convex rolls (mm).

x-coordinate	Roll gap value							
	r_d = 10	r_d = 8	r_d = 6	r_d = 4	r_d = 2	r_d = -2	r_d = -4	r_d = -6
0 (middle)	2.650	2.650	2.650	2.650	2.650	2.700	2.700	2.700
10	2.652	2.652	2.651	2.650	2.650	2.699	2.698	2.698
20	2.658	2.656	2.654	2.651	2.649	2.695	2.693	2.691
30	2.668	2.663	2.658	2.653	2.648	2.689	2.684	2.679
40 (side)	2.683	2.673	2.665	2.656	2.647	2.680	2.671	2.662
Difference between x=0 and x=40	-0.033	-0.023	-0.015	-0.006	0.003	0.02	0.029	0.038
Longitudinal curvature radius	253	239	268	623	1068 (reverse direction)	219 (reverse direction)	168 (reverse direction)	160 (reverse direction)

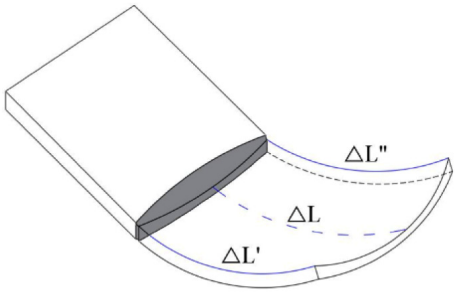

(a)

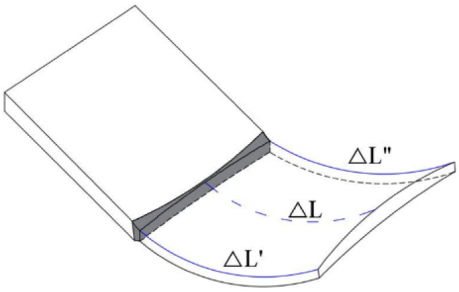

(b)

Fig. 3. The forming process when the distribution rule of roll gap is non-uniform: (a) narrow in the middle and wide on both sides; (b) wide in the middle and narrow on both sides.

spherical sheet. If the roll gap distribution rule is wide in the middle and narrow on both sides, the elongation of metal fiber on two sides will be larger than that in the middle, namely, $\Delta L < \Delta L'$, $\Delta L < \Delta L''$. The curved surface deforms in the opposite directions along the cross-section lines in the two principal directions, resulting in a saddle part.

The bending of the formed sheet in TSRRAR occurs after the non-uniform deformation generated by a specific distribution of roll gap. This non-uniform deformation is mainly reflected in the difference of longitudinal strain generated in various positions of the formed sheet. The additional internal stress formed between adjacent metal fibers with different longitudinal elongations causes non-uniform deformation. The content of additional internal stress is discussed in detail in Sec. 4.2.

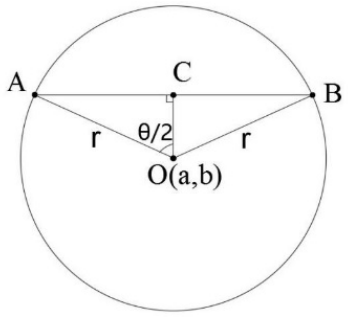

Fig. 4. Schematic diagram of arc length fitting.

3. Process control method

In order to realize the control of the 3D surface rolling process, it is necessary to analyze the longitudinal flow of the metal inside the formed sheet with different maximum compression rate, which can be represented by the distribution of longitudinal strain and the change of longitudinal arc length. It is easy to obtain the longitudinal strain result through numerical simulation, whereas the longitudinal arc length needs to perform circle arc fitting on the longitudinal arc of the formed sheet adopting the user-defined curve fitting algorithm in Origin 2018. The premise of curve fitting is that the accuracy of the formed sheet satisfies the longitudinal arc on the concave surface is a precise circle arc.

First, the node coordinates (x, y) on the longitudinal arc along the longitudinal and thickness direction are fitted, and the fitting equation is $y = b + \left(r^2 - (x-a)^2\right)^{1/2}$, where a and b are the center coordinates of the fitted circle; r is the radius of the fitted circle. After assigning initial values to a, b, and r, respectively, their fitted value can be obtained. According to the coordinate values of the starting point A and the end point B of the circle arc, the value of AC can be obtained by the length of the chord AB. As shown in Fig. 4, in the right triangle AOC

$$\sin\frac{\theta}{2} = \frac{AC}{r}. \quad (1)$$

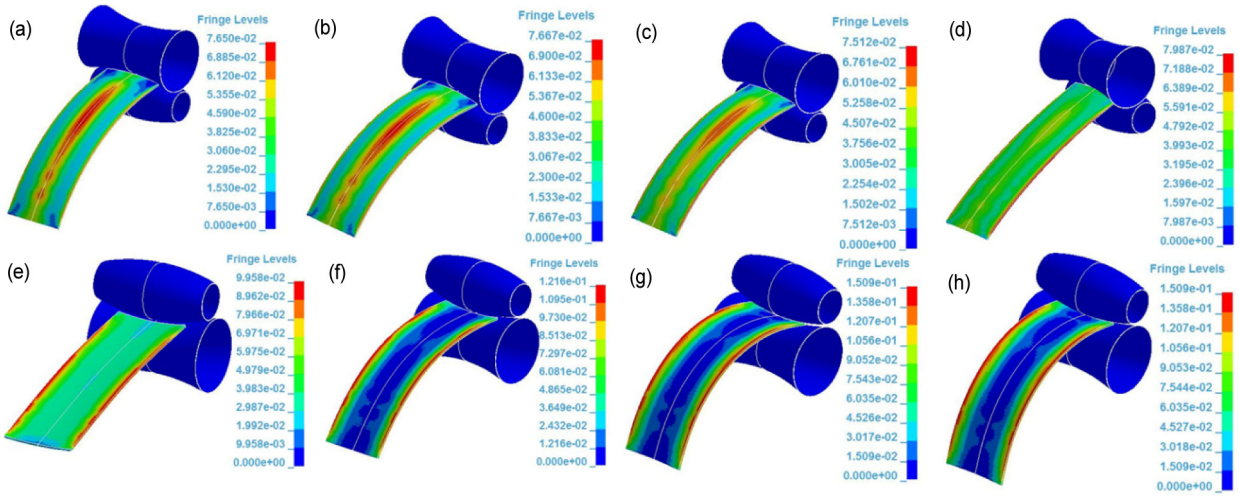

Fig. 5. Plastic strain distribution of the formed sheet with various differences in axial radius of roller.

Therefore, in the sector AOB

$$L_{\widehat{AB}} = r \cdot \theta . \tag{2}$$

According to Eqs. (1) and (2), the longitudinal arc length of the formed sheet can be calculated with different distributions of roll gaps.

Thickness reduction, transverse bending and longitudinal extension co-exist when the sheet is deformed. Since the roll gap is uneven, the elongation of metal at different positions in the transverse direction of the formed sheet is also different. It is assumed that the length of the metal fiber after deformation with an initial length ΔL_0 at the point s is $\Delta L(s)$, and the longitudinal strain increment is $d\varepsilon_L(s) = d(\Delta L)/\Delta L$. Since the main direction of strain remains unchanged during deformation, the total longitudinal strain at point s is

$$\varepsilon_L(s) = \int_{\Delta L_0}^{\Delta L} \frac{d(\Delta L)}{\Delta L} = \ln \frac{\Delta L(s)}{\Delta L_0} . \tag{3}$$

After the process of 3D surface rolling, the longitudinal fiber length of the metal with an initial length ΔL_0 at the point s is

$$\Delta L(s) = \Delta L_0 \exp\left[\varepsilon_L(s)\right] . \tag{4}$$

TSRRAR is a process dominated by compression deformation and with large plastic deformation, so the elastic deformation can be ignored. According to the condition of constant volume, the strain at a point in the sheet satisfies

$$\varepsilon_T + \varepsilon_L + \varepsilon_\delta = 0 \tag{5}$$

where ε_T is the transverse strain; ε_L the longitudinal strain; ε_δ the strain in the thickness direction.

The deformation of the formed sheet in 3D surface rolling is mainly reflected in the thickness reduction and the longitudinal elongation, whereas the width of the formed sheet changes little. Therefore, the lateral spread can be ignored during deformation analysis, namely $\varepsilon_T \approx 0$. Since the thickness of the formed sheet is obviously smaller than its length and width, the strain distribution along the thickness direction is assumed to be uniform. Thus

$$\varepsilon_L(s) = -\varepsilon_\delta(s) = -\ln \frac{\delta(s)}{\delta_0} \tag{6}$$

where δ_0 is the initial thickness of the sheet before deformation; $\delta(s)$ the thickness at the point s on the curved surface after deformation.

If the influence of elastic deformation and work hardening on the forming result is not considered, the thickness $\delta(s)$ after deformation and the roll gap distribution function $h(s)$ at point s on the curved surface are the same, so the relationship between longitudinal strain and roll gap distribution function is

$$h(s) = \delta_0 \exp\left[-\varepsilon_L(s)\right] . \tag{7}$$

Eqs. (4) and (7) show that the longitudinal strain of the formed sheet depends on the roll gap distribution, and the roll gap distribution directly determined by process parameters affects the longitudinal arc length. Therefore, the longitudinal strain and longitudinal arc length of the formed sheet are analyzed to understand the TSRRAR process and realize the shape control of the formed sheet.

4. Numerical simulation of the TSRRAR process

4.1 Finite element model and the selection of axial radius of roller

Finite element models of spherical and saddle shapes estab-

Table 2. Material properties of Al1060-O.

Material properties	Value
Density (kg/m^3)	2705
Elastic modulus (GPa)	69
Poisson's ratio	0.33
Yield strength (MPa)	28
Tangent modulus (MPa)	48

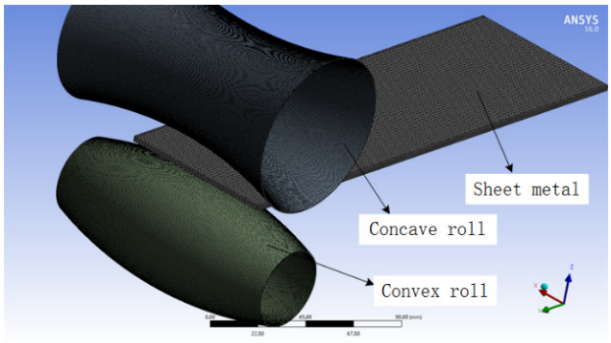

Fig. 6. Finite element model.

lished by ANSYS Workbench environment were used to study the influence of the axial radius of roller on the type of surface, the mechanics of longitudinal deformation, the variable range of longitudinal curvature radius of the formed sheet produced only by one group of rollers, and the variation in forming force.

Fig. 6 shows that the convex roll, the concave roll and the sheet metal adopt solid elements. The mesh size of the roller is set to be 0.6 mm, and so does that of the longitudinal direction of the formed sheet after the mesh refinement process considering the calculating time and precision. The mesh size in the transverse direction is defined as 1.8 mm to reduce the calculating time. There are three layers in the thickness direction for a better bending analysis and the initial dimensions (length × width × thickness) of the sheet are 250 × 80 × 2.7 mm.

Aluminum 1060-O is used in the simulation and Table 2 shows the material properties. The sheet metal conforms to the elastoplastic constitutive relationship with bilinear isotropic hardening. The static friction coefficient is 0.1, and the dynamic friction coefficient is 0.05. Since the analysis is mainly about the sheet metal, rollers are defined as rigid bodies and to be hollow, and the difference of torus radii is 0.5 mm. After all finite element model settings are completed, a keyword file is created, and the LS-DYNA solver is adopted for explicit dynamic analysis.

Table 1 lists the roll gap values with various differences in axial radius of concave and convex rolls. The axial radius of the concave roll is 216 mm with $r_d > 0$, and the axial radius of the convex roll is 216 mm with $r_d < 0$. The relationship between the roll gap distribution and the curvature radius of formed sheet is complicated in the SFR method. With the adoption of rigid arc-shaped rollers, the roll gap distribution function in SFR is simplified to two constants in TSRRAR, the axial radius of roller and the maximum reduction. That is to say, the relationship between the axial radius of roller and the longitudinal curvature radius of the formed sheet can be regarded as a one-variable function. It reflects the flexibility of this forming method as well as the reduction does if the new device in Fig. 2 is adopted.

Table 3. Roll gaps with different maximum reduction rates and differences in axial radius of roller.

Number of roll gap	Maximum reduction rate	r_d /mm
a	1 %	6
b	1.5 %	6
c	2 %	6
d	1 %	10
e	1.5 %	10
f	2 %	10

The corresponding results in Fig. 5 indicate that the plastic strain of saddle sheets in the middle is smaller than that on both sides, while it is the opposite of spherical sheets, which results from the difference of roll gap value between the middle and sides of the formed sheet. Besides, the relationship mentioned above is not monotonic and the maximum longitudinal deformation occurs with r_d = 8 mm. There is a matching problem between process parameters, which affects the longitudinal deformation range of formed sheet if only using one group of rollers.

The selection of axial radius of roller is mainly based on the transverse curvature radius of the target profile, 216 mm. Since the axial radius of roller is newly found to be similar to the transverse curvature radius of the formed sheet in the proposed technology (see Table 4), 216 mm is defined as the concrete value of axial radius of the concave roll.

As described above, there is a matching problem between process parameters. Based on the simulation and experimental experience, the difference in axial radius of roller of nearly 6 mm is reasonable for the sheet width applicable to this device. For comparison, the concrete values of axial radius of the convex roll are selected to be 206 and 210 mm in this study.

4.2 Mechanical analysis of longitudinal deformation

As described above, two combinations of the axial radius of roller are selected to study the longitudinal strain and stress field of the spherical sheet, thereby exploring the mechanical mechanism of longitudinal deformation in the process of TSRRAR. Simulation conditions for mechanical analysis include three maximum reduction rates of 1, 1.5 and 2 % (see Table 3), and the number of roll gap corresponds to the number of simulation results in Figs. 7 and 9.

The level of maximum reduction rate is obviously smaller than conventional cold rolling under the tension force that produces the overall deformation. Particularly, the level of reduc-

Table 4. The curvature radii and longitudinal arc length of simulated sheets when the roll gap distribution varies (mm).

r_d	Maximum reduction	Transverse curvature radius	Longitudinal curvature radius	Longitudinal arc length in the middle of formed sheet		
				Concave surface	Convex surface	Difference value
6	0.027	214.9	564	250.81	252.05	1.24
6	0.034	214.5	320	251.52	253.61	2.09
6	0.041	213.0	259	252.61	255.15	2.54
6	0.047	212.9	228	253.93	256.82	2.89
10	0.027	203.9	688	251.29	251.62	0.33
10	0.034	204.6	344	252.24	253.19	0.95
10	0.041	201.8	227	253.53	255.09	1.56
10	0.047	197.1	172	255.21	257.32	2.11

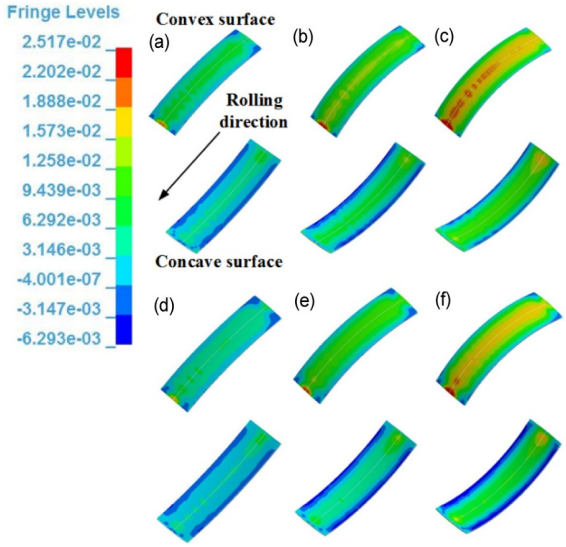

Fig. 7. Distribution of longitudinal strain of formed sheet when the roll gap varies.

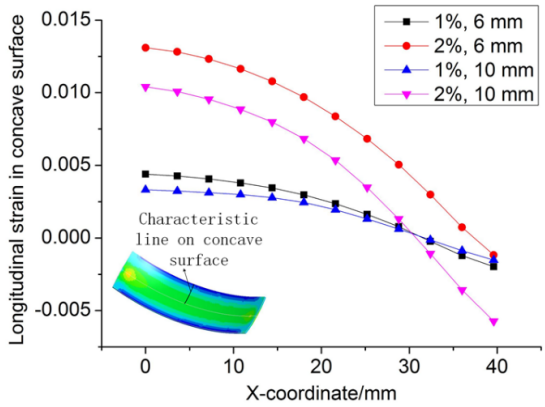

Fig. 8. Diagram of longitudinal strain along characteristic line on concave surface of formed sheet when the roll gap varies.

tion in the simulation is smaller than that in the experiment in this study due to the high precision of the size and shape of roller. The roundness of the experimental roller is between 0.01 and 0.02 mm, which significantly decreases the non-uniform deformation degree of the formed sheet.

In fact, it is an advantage that a relatively small reduction is required in forming 3D surface parts, because the forming part with a slight thickness change will benefit to the subsequent process when used as a weldment owing to an easier matched cross section, and reduce the forming force to realize the energy-saving production.

Fig. 7 shows the distribution of longitudinal strain of formed sheets when the roll gap varies. With the maximum reduction rate increasing from 1 to 2 %, the maximum values of longitudinal strain with r_d = 6 and 10 mm become larger from 0.021 to 0.030 and from 0.019 to 0.028, respectively. It can be intuitively seen from this figure that the longitudinal deformation of the formed sheet depends on the value of the longitudinal strain. In addition, when the difference in axial radius of roller is small, the increasing rate of the roll gap value from the middle to both sides is also slow, so the longitudinal elongation of the metal is large at the same position of the sheet. Thus, the longitudinal strain will increase with the decreased difference in axial radius of roller if the maximum reduction rate remains the same.

Fig. 8 shows a detailed comparison on longitudinal strain along the characteristic line of transverse direction. The strain value regularly decreases from the middle to both sides, indicating that the compressed metal flows more obviously along the longitudinal direction with the narrow roll gap or the large maximum reduction.

On the premise of ensuring that the maximum roll gap is approximately equal to the sheet thickness, the difference in axial radius of roller represents the degree of non-uniform deformation of the sheet. Additionally, the non-uniform deformation of formed sheet is mainly reflected in the stepwise change of the longitudinal strain along the transverse direction, and this distribution characteristics should be obtained to ensure the effectiveness of the simulation result.

Fig. 9 shows the distribution of longitudinal stress in condition that the roll gap distribution of 3D surface rolling is narrow in the middle and wide on both sides. The number and colors indicate the stress magnitude on the formed sheet metal, and six simulation results of longitudinal stress are assigned to be

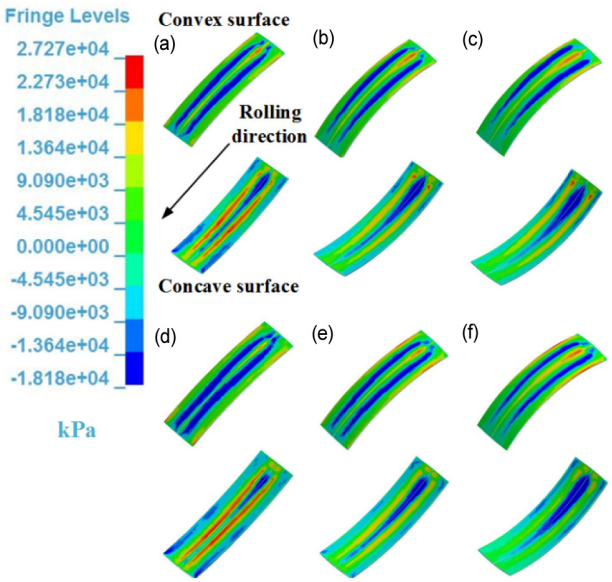

Fig. 9. Distribution of longitudinal stress of formed sheet when the roll gap varies.

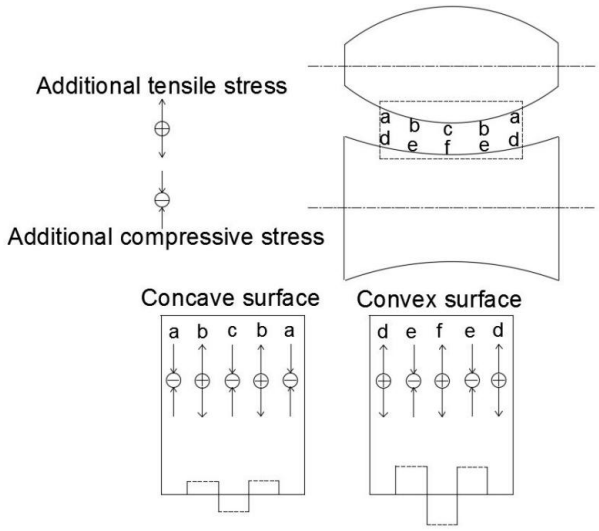

Fig. 10. Mechanical mechanism of the longitudinal deformation for the spherical sheet.

the same magnitude for easy comparison. There is an obvious phenomenon from the distribution diagram that the longitudinal stress value at the center and both sides on the concave surface of the formed sheet is negative, and that in the middle of these two positions is positive; whereas the type of longitudinal stress on the convex surface of the formed sheet is the opposite. Since the sheet is a whole, the non-uniform deformation is limited, and the mutually balanced longitudinal stress is formed between adjacent metals, which is called the additional stress.

The reaction between adjacent metals on the concave surface is discussed as an explanation for the distribution of additional stress. The deformation degree of the metal part b of the sheet is relatively small, whereas the deformation degree of the metal part c in the middle is relatively large. If the parts b and c do not belong to the same whole, the metal in the middle will elongate more in the longitudinal direction than the adjacent metal on both sides (see the dotted line in Fig. 10). However, the sheet is a whole, and the metal of the two parts b and c cannot be freely extended with mutual restriction. The free extension of the metal part c is restricted by the metal part b to be compressed, and the metal part b is stretched by the metal part c to be tensioned. Therefore, the balanced internal stress is generated, with additional compressive stress in the middle, and additional tensile stress in the adjacent areas of the middle part. Also, the force on both sides of the sheet metal only comes from the action of adjacent metal on one side, so the stress is opposite to that of the adjacent metal, that is, the addition compressive stress.

The above analysis shows that the additional stress is the internal force generated for maintaining the integrity and continuity of the sheet to restrict the non-uniform deformation. Thus, it is the additional stress that causes a flat sheet to perform the longitudinal bending deformation, which is the mechanical mechanism of the longitudinal deformation of TSRRAR.

4.3 Influence on the longitudinal arc length

After the profiles of rollers on the middle section along the transverse direction are processed into the circle arc shape, the roll gap and its distribution values can be generated by two process parameters, the axial radius of roller and the maximum compression rate. In the process of 3D surface rolling, the transverse curvature radius of the formed sheet can be directly determined by the axial radius of roller. Nevertheless, the control of longitudinal curvature radius is more complicated, and it needs to be realized by exploring the influence law between the roll gap distribution and longitudinal bending deformation of the formed sheet.

Table 4 shows the results of longitudinal curvature radius on the concave surface of the formed sheet, and the longitudinal arc length on the concave and convex surfaces in the middle of the formed sheet under different conditions of the roll gap distribution. The calculation examples meet the requirements of forming accuracy, namely the longitudinal arc can be directly fitted to a circle arc with high precision to obtain the curvature radius required to calculate the arc length.

It can be seen from the table that if the maximum reduction is the same, the difference of longitudinal arc length on the convex and concave surfaces with r_d = 6 mm will be larger than that with r_d = 10 mm. It means metal fibers inside the formed sheet also possess uneven elongation along the thickness direction, but the degree of this unevenness is not directly related to the magnitude of longitudinal bending deformation. As for the same combination of the axial radius of roller, a 3D surface part with a greater longitudinal arc length possesses larger deformation in longitudinal direction. Thus, the longitudinal arc length is found to be indicative of longitudinal deformation when the axial radius of roller remains the same.

Table 5. Forming results when the roll gap distribution varies.

No.	r_d /mm	Experimental sheet		Simulation sheet		
		Maximum compression rate/%	Longitudinal curvature radius/mm	Maximum compression rate/%	Longitudinal curvature radius/mm	Maximum resultant force/KN
①	6	2.22	456	2.30	450	2.27
②	6	2.93	304	2.96	302	2.59
③	6	3.59	214	3.59	207	2.89
④	6	4.22	178	4.15	188	3.07
⑤	6	5.11	167	5.11	164	3.40
⑥	10	1.30	358	1.33	361	1.60
⑦	10	1.96	222	1.78	246	1.86
⑧	10	2.48	180	2.52	176	2.21
⑨	10	3.15	148	3.26	143	2.55
⑩	10	3.89	130	3.70	129	2.77

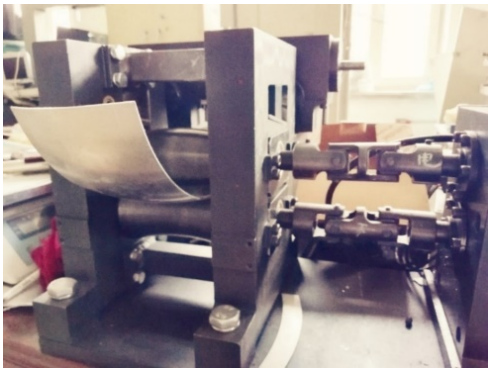

Fig. 11. Forming process of TSRRAR and the experimental device.

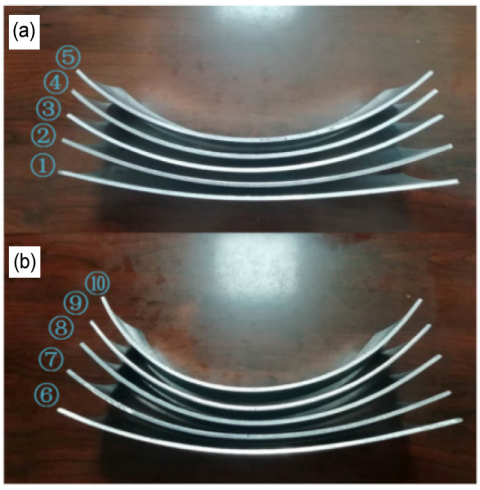

Fig. 12. Experimental sheets when the roll gap distribution varies: (a) r_d = 6 mm; (b) r_d = 10 mm.

5. Experimental results and discussion

5.1 Forming device and spherical results

Fig. 11 shows the forming process of 3D surface rolling for a spherical sheet. The device can form the sheet within a width of 120 mm. Fig. 12 shows the experimental sheets produced by two pairs of rollers. For the first pair, the axial radii are 210 mm for the convex roll and 216 mm for the concave roll; for the other pair, the axial radii are 206 mm for the convex roll and 216 mm for the concave roll. The initial dimensions (length × width × thickness) of the sheet are 250 × 80 × 2.7 mm, and the maximum compression rates are different.

Table 5 shows the measured longitudinal curvature radius on the concave surface of spherical sheets with r_d = 6 and 10 mm. Nos. ④ and ⑧ show that if the difference in axial radius of roller changes from 6 to 10 mm, the required maximum compression rate will decrease from 4.22 to 2.48 % with the same longitudinal curvature radius (179 mm) to be obtained, which means the bigger the difference in axial radius of roller, the larger the degree of non-uniform deformation generated by inhomogeneous compression. The longitudinal curvature radius of the formed sheet decreases with the increased maximum compression rate. This phenomenon can be understood from the principle of TSRRAR that the deformation of the inner metal of formed sheet along the longitudinal direction becomes more evident after increasing the compression rate, thereby increasing the degree of bending. Besides, the corresponding simulation result of maximum resultant force with Nos. ④ and ⑧ decreases from 3.07 to 2.21 KN with the same target profile to be obtained, demonstrating that the difference in axial radius of roller affects the forming force. Therefore, it can be more labor-saving to obtain a target profile and the forming difficulty can be effectively reduced by selecting the difference in axial radius of roller, which makes this technology with slightly bending rollers in the future study not only be more flexible, but also be benefit to the energy-saving production.

5.2 Influence on the type of shape and longitudinal deformation range of the formed sheet

Fig. 13 shows the forming results of saddle and spherical

Table 6. Roll gap values along the transverse direction of the formed sheet while the reduction in the middle is 0.027 mm (mm).

Distance from horizontal center	Roll gap value	
	r_d = 2 mm	r_d = 6 mm
0 (middle)	2.673	2.673
10	2.672	2.677
20	2.670	2.688
30	2.666	2.706
40 (side)	2.661	2.732
Difference between middle and side	0.012	-0.059

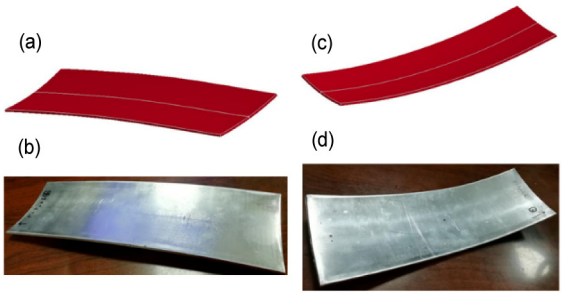

Fig. 13. Forming results while the difference of axial radius of roller is positive: (a) a simulation result with r_d = 2 mm; (b) an experimental sheet with r_d = 2 mm; (c) a simulation result with r_d = 6 mm; (d) an experimental sheet with r_d = 6 mm.

sheets with r_d = 2 and 6 mm, which indicates that the forming results are not all spherical sheets when the axial radius of the convex roll is smaller than that of the concave roll. That is to say, the decisive factor that affects the sheet shape is not the sign (positive or negative) of the difference in axial radii of the convex and concave rolls.

Table 6 shows the roll gap distribution corresponding to the results in Fig. 13. The initial dimensions (length × width × thickness) of the sheets are 250 × 80 × 2.7 mm. The difference between the middle and two sides of the roll gap is 0.012 mm if r_d = 2 mm, and the forming result is a saddle sheet. Nevertheless, if the sheet size remains the same and r_d = 6 mm, the difference between the middle and two sides of the roll gap is -0.059 mm, resulting in a spherical sheet. Therefore, it is the difference between the middle and two sides of the roll gap that directly determines the shape type of formed sheet. If the difference is less than 0 mm, the forming results are spherical sheets, and the opposite are saddle ones.

With the maximum reduction increases by 0.02 mm, two saddle sheets with significantly different longitudinal deformation are obtained in Fig. 14, meaning that the TSRRAR process only needs a slight change on thickness of the formed sheet to generate bidirectional bending deformation. The initial dimensions (length × width × thickness) of the sheets are 330 × 80 × 2.4 mm. As shown in Fig. 14(a), the plastic strain distribution of the sheet on both sides is greater than that in the middle, which makes the metal fibers of two sides elongate and forms a saddle-shaped surface.

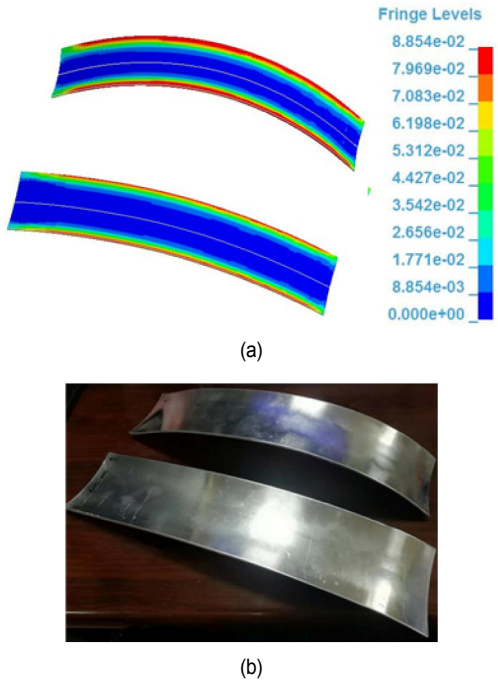

Fig. 14. Forming results with r_d = -2 mm: (a) plastic strain distribution of simulation parts; (b) experimental sheets.

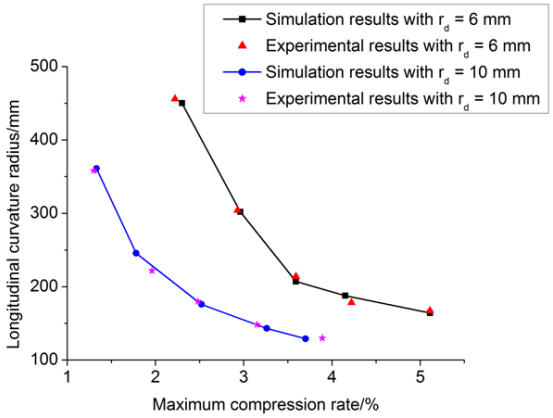

Fig. 15. The longitudinal curvature radius of the simulated and experimental sheet when the roll gap distribution varies.

Fig. 15 shows the variation range of the longitudinal curvature radius of simulated and experimental sheets with different maximum compression rates and r_d. Different combinations of the axial radius of roller produce various shapes of 3D surface parts with r_d = 6 mm exhibiting a greater longitudinal curvature radius of the formed sheet than r_d = 10 mm if the compression remains the same. When the maximum compression rate varies from 2.22 to 5.11 % and from 1.30 to 3.89 %, the variation range of longitudinal curvature radius with r_d = 6 and 10 mm is from 167 to 456 mm, and from 130 to 358 mm, respectively. Moreover, as the maximum compression rate increases, the changing trend of the longitudinal curvature radius of the formed sheet is from fast to slow. After the maximum

compression rate reaches 4.22 % with r_d = 6 mm (or 3.15 % with r_d = 10 mm), the change of the longitudinal curvature radius is insignificant if the compression rate continues to rise.

The principle of 3D surface rolling is the bidirectional bending deformation after uneven elongation caused by inhomogeneous compression, and the compression action is only influenced by the maximum compression rate without changing rollers. Thus, it is feasible to use only one group of rollers to effortlessly produce various shapes of formed sheets and the difference in axial radius of roller affects the longitudinal deformation range.

6. Conclusions

3D surface rolling with rigid arc-shaped rollers is a novel flexible forming method of 3D surface sheet metal parts, and it is more practicable of the non-uniform deformation principle adopted in TSRRAR than that in SFR to realize the 3D surface forming. Numerical simulations and experiments are carried out to investigate the forming ability of the TSRRAR technology without changing rollers. The conclusions are summarized as follows:

1) It is feasible to use only one group of rollers to effortlessly produce various shapes of formed sheets. When the maximum compression rate varies from 2.22 to 5.11 % and from 1.30 to 3.89 %, the variation range of longitudinal curvature radius with r_d = 6 and 10 mm is from 167 to 456 mm, and from 130 to 358 mm, respectively.

2) The difference in axial radius of roller affects the forming force. If the difference in axial radius of roller changes from 6 to 10 mm, the maximum resultant force will decrease from 3.07 to 2.21 KN, and the required maximum compression rate will decrease from 4.22 to 2.48 % with the same longitudinal curvature radius (179 mm) to be obtained, meaning that the forming difficulty can be effectively reduced by selecting the difference in axial radius of roller.

Nomenclature

r : Axial radius of roller
r_d : Difference in axial radii of the concave and convex rollers
$L_{\overline{AB}}$: Length of circle arc AB
$\varepsilon_L(s)$: Total longitudinal strain at point S
δ_0 : Initial thickness of sheet
$\delta(s)$: Thickness at point S
$h(s)$: Roll gap distribution function

References

[1] M. Z. Li, K. Nakamura, S. Watanabe and K. Sugawara, Study of the basic principles (1st report: research on multi-point forming for sheet metal), *Proceedings of the Japanese Spring Conference for Technology of Plasticity* (1992) 519-522.

[2] M. Tera, R. E. Breaz, S. G. Racz and C. E. Girjob, Processing strategies for single point incremental forming—a CAM approach, *The International Journal of Advanced Manufacturing Technology*, 102 (5) (2019) 1761-1777.

[3] B. Zhou, X. Han, S. K. Tan, Y. Liu and Z. Wei, Numerical and experimental study on plate forming using the technique of line heating, *International Journal of Maritime Engineering*, 156 (2014) 265-275.

[4] A. Tolipov, A. Elghawail, M. Abosaf, D. Pham, H. Hassanin and K. Essa, Multipoint forming using mesh-type elastic cushion: modelling and experimentation, *The International Journal of Advanced Manufacturing Technology*, 103 (5-8) (2019) 2079-2090.

[5] Y. H. Seo, B. S. Kang and J. Kim, Study on relationship between design parameters and formability in flexible stretch forming process, *International Journal of Precision Engineering and Manufacturing*, 13 (10) (2012) 1797-1804.

[6] S. J. Yoon and D. Y. Yang, Development of a highly flexible Incremental roll forming process for the manufacture of a doubly curved sheet metal, *CIRP Annals*, 52 (1) (2003) 201-204.

[7] R. J. Li, M. Z. Li, N. J. Qiu and Z. Y. Cai, Surface flexible rolling for three-dimensional sheet metal parts, *Journal of Materials Processing Technology*, 214 (2) (2014) 380-389.

[8] D. M. Wang, M. Z. Li and Z. Y. Cai, Continuous-forming method for three-dimensional surface parts combining rolling process with multipoint-forming technology, *The International Journal of Advanced Manufacturing Technology*, 72 (1) (2014) 201-207.

[9] S. J. Yoon and D. Y. Yang, An incremental roll forming process for manufacturing doubly curved sheets from general quadrilateral sheet blanks with enhanced process features, *CIRP Annals*, 54 (1) (2005) 221-224.

[10] D. S. Shim, D. Y. Yang, K. H. Kim, S. W. Chung and M. S. Han, Investigation into forming sequences for the incremental forming of doubly curved plates using the line array roll set (LARS) process, *International Journal of Machine Tools and Manufacture*, 50 (2) (2010) 214-218.

[11] Z. Y. Cai and M. Z. Li, Principle and theoretical analysis of continuous roll forming for three-dimensional surface parts, *Science China Technological Sciences*, 56 (2) (2013) 351-358.

[12] Z. Y. Cai, M. Z. Li and Y. W. Lan, Three-dimensional sheet metal continuous forming process based on flexible roll bending: principle and experiments, *Journal of Materials Processing Technology*, 212 (1) (2012) 120-127.

[13] M. Z. Li, Z. Y. Cai, R. J. Li, Y. W. Lan and N. J. Qiu, Continuous forming method for three-dimensional surface parts based on the rolling process using bended roll, *Journal of Mechanical Engineering*, 48 (14) (2012) 44-49 (in Chinese).

[14] N. J. Qiu, M. Z. Li and R. J. Li, The shape analysis of three-dimensional flexible rolling method, *Proceedings of the Institution of Mechanical Engineers Part B: Journal of Engineering Manufacture*, 230 (4) (2016) 618-628.

[15] J. S. Yoon, S. E. Son, W. J. Song, J. Kim and B. S. Kang, Study on flexibly-reconfigurable roll forming process for multi-curved surface of sheet metal, *International Journal of Precision Engineering and Manufacturing*, 15 (6) (2014) 1069-1074.

[16] J. S. Yoon, J. Kim, H. H. Kim and B. S. Kang, Feasibility study

on flexibly reconfigurable roll forming process for sheet metal and its implementation, *Advances in Mechanical Engineering*, 6 (2014) 958925.

[17] J. S. Yoon, J. Kim and B. S. Kang, Deformation analysis and shape prediction for sheet forming using flexibly reconfigurable roll forming, *Journal of Materials Processing Technology*, 233 (2016) 192-205.

[18] X. T. Wang and M. Z. Li, Research on three-dimensional curved surface rolling based on rigid arc-shaped rollers, *The International Journal of Advanced Manufacturing Technology*, 107 (1) (2020) 805-814.

[19] S. Torsakul and N. Kuptasthien, Effects of three parameters on forming force of the single point incremental forming process, *Journal of Mechanical Science and Technology*, 33 (6) (2019) 2817-2823.

[20] J. Wang, L. Li and H. Jiang, Effects of forming parameters on temperature in frictional stir incremental sheet forming, *Journal of Mechanical Science and Technology*, 30 (5) (2016) 2163-2169.

[21] T. Zhang, H. Sha, S. Lu, C. Du and P. Chen, Study on flexible two-axis roll-bending process for component with non-circular section, *Journal of Mechanical Science and Technology*, 33 (9) (2019) 4421-4429.

Xintong Wang is a Ph.D. student in the College of Materials Science and Engineering at Jilin University. He received his B.S. from Roll Forging Research Institute at Jilin University. His research field is flexible plastic forming of sheet metal.

Mingzhe Li is currently a Professor in the College of Materials Science and Engineering at Jilin University. He received his B.S. and M.S. degrees from Jilin University of Technology, Changchun, China in 1977 and 1981, respectively. He then obtained his Ph.D. degree from Nagaoka University of Technology, Japan in 1990. Prof. Li's primary research interests include flexible plastic forming and digital manufacturing of sheet metal.